

The signature amidase from *Sulfolobus solfataricus* belongs to the CX₃C subgroup of enzymes cleaving both amides and nitriles

Ser195 and Cys145 are predicted to be the active site nucleophiles

Elisa Cilia^{1,2}, Armando Fabbri¹, Monica Uriani¹, Giuseppe G. Scialdone¹ and Sergio Ammendola^{1,2}

¹ Centre of Biotechnology-Bioprogress, Anagni, Italy

² AMBIOTEC SAS SS7, Cisterna di Latina, Italy

Keywords

amidase; catalytic triad; CX₃C; modelling; mutagenesis

Correspondence

S. Ammendola, Via Paduni 240-03012
Anagni FR, Italy
Fax: +39 077 576 6541
Tel: +39 077 576 6824
E-mail: sergio.ammendola@fastwebnet.it

(Received 14 June 2005, revised 18 July 2005, accepted 28 July 2005)

doi:10.1111/j.1742-4658.2005.04887.x

The signature amidase from the extremophile archeum *Sulfolobus solfataricus* is an enantioselective enzyme that cleaves S-amides. We report here that this enzyme also converts nitriles in the corresponding organic acid, similarly to the well characterized amidase from *Rhodococcus rhodochrous* J1. The archaeal and rhodococcal enzymes belong to the signature amidases and contain the typical serine-glycine rich motif. They work at different optimal temperature, share a high sequence similarity and both contain an additional CX₃C motif. To explain their dual specificity, we built a 3D model of the structure of the *S. solfataricus* enzyme, which suggests that, in addition to the classical catalytic Ser-cisSer-Lys, a putative additional Cys-cisSer-Lys catalytic site, likely to be responsible for nitrile hydrolysis, is present in these proteins. The results of random and site-directed mutagenesis experiments, as well as inhibition studies support our hypothesis.

Amide hydrolase (AH) and nitrilase (Nit) are two superfamilies of enzymes cleaving C–N bonds of different substrates [1]. These proteins all share the typical α/β hydrolase fold and can be grouped on the basis of their catalytic site and preferred substrate [2,3]. The enzymes of the Nit superfamily have a catalytic site formed by a Glu–Cys–Lys triad and can hydrolyse nitriles (EC 3.5.1.1) or the carboxylic amide group (EC 3.5.1.4) [4].

The AH superfamily includes the signature amidases, originally identified by primary structure analysis [5]. The substrate specificities and biological functions of these enzymes vary widely, but it has been shown that they all have a similar catalytic mechanism mediated by a Ser–cisSer–Lys catalytic triad [6–8].

Recently, the gene coding for the signature amidase from *Sulfolobus solfataricus* (SsAH) has been expressed in *Escherichia coli* and characterized [9]. This is a wide spectrum AH, converting carboxylic amides to their

corresponding organic acids. We report that the SsAH enzyme also possesses nitrilase activity, a property shared by the well-characterized signature amidase from *Rhodococcus rhodochrous* J1 (RhorhJ1) [10,11]. Both enzymes contain an additional CX₃C motif.

To understand the structural basis of this dual specificity, we constructed random mutants of SsAH and screened them for their activity on amide, nitrile and ester substrates. Mutants showing increased activity on nitriles all carried the Lys96Arg substitution, an observation confirmed by site-directed mutagenesis.

The structural framework of the observed mutations was investigated by constructing a homology model of the enzyme. The model suggests that a putative additional catalytic triad formed by Ser171–Cys145–Lys96, where position 145 corresponds to the second cysteine of the additional CX₃C motif, exists in this enzyme. We suggest that this alternative active site is responsible for the hydrolysis of nitriles, with Cys145 acting

Abbreviations

AH, amide hydrolase; Nit, nitrilase; RhorhJ1, *Rhodococcus rhodochrous* J1; SH, serine hydrolase; Ss, *Sulfolobus solfataricus*; WT, wild type.

as the nucleophile involved into the thiol-mediated catalysis of nitriles.

Sequence analysis suggests that other signature amidases, containing the additional CX₃C motif, constitute a subgroup of the family and might all be able to cleave both amides and nitriles.

Results

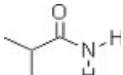
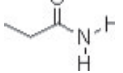
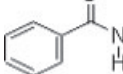
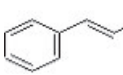
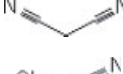
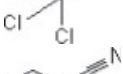
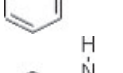
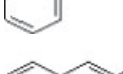
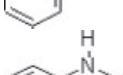
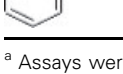
Recently, the recombinant wild-type gene coding for the signature SsAH protein (SsAH-WT) has been cloned in *E. coli* and its product characterized. The enzyme exhibits high thermostability and thermophilicity [9]. The archeal enzyme converts several amide substrates in their corresponding organic acids producing stoichiometric amounts of NH₃ (data not shown). Consistent with previously published data, our preparation of the purified recombinant SsAH-WT remains

active at 70 °C for about 6 days and has a half-life of 5 h at 95 °C (data not shown).

We found that SsAH-WT is able to convert both amides and nitriles, and in particular benzonitrile (Table 1). The specific activity of the enzyme on the Benzonitrile substrate is about 1/2000 with respect to its activity on benzamide ($6 \times 10^{-4} \mu\text{mol}\cdot\text{min}^{-1}\cdot\text{mg}^{-1}$ and $1.18 \mu\text{mol}\cdot\text{min}^{-1}\cdot\text{mg}^{-1}$, respectively). This is similar to the observations for RhorhJ1, where the ratio between the two activities is about 1/6000 [11].

A sequence alignment of signature AHs, shown in Fig. 1, highlights blocks of structurally conserved residues. These include the strictly conserved GSSXG motif. The first serine in this motif (Ser171 using SsAH numbering) forms the catalytic triad, together with Lys96 and Ser195 [12]. The second pattern, Cys141X₃Cys145, is conserved only in a limited num-

Table 1. Kinetic parameters of SsAH-WT and SsAH-K96R on different substrates. na, activity undetectable.

Structure	Substrate	SsAH-WT		SsAH-K96R	
		K_M (μmol)	k_{cat} s ⁻¹	K_M (μmol)	k_{cat} s ⁻¹
	Isobutyramide ^a	0.099	175	0.2	160
	Propionamide ^a	0.102	181	0.093	160
	Benzamide ^b	0.674	1192	0.723	1246
	Cinnamamide ^b	0.434	769	0.526	906
	Malononitrile ^b	0.0795×10^{-3}	0.140	0.609×10^{-3}	1.05
	Trichloroacetonitrile ^a	0.5×10^{-6}	0.010	0.130×10^{-3}	0.225
	Benzonitrile ^b	0.005	0.088	0.006	
	Phenylglycinenitrile	0.024×10^{-3}	0.043	9×10^{-6}	0.016
	Cinnamonitrile ^a	na	na	9.607×10^{-6}	0.016
	3-Anilinopropionitrile ^a	0.157×10^{-3}	0.279	0.103×10^{-3}	0.177

^a Assays were carried at pH 7.4 and T = 70 °C using 61 μg purified protein. Activity was measured with the Berthelot assay, by reading the absorbance of the colour developed at $\lambda = 630 \text{ nm}$. ^b Benzamide and benzonitrile values were determined by HPLC.

Shaded regions correspond to predicted or observed elements of secondary structure. Light gray = alpha helices, darker gray = beta strands.

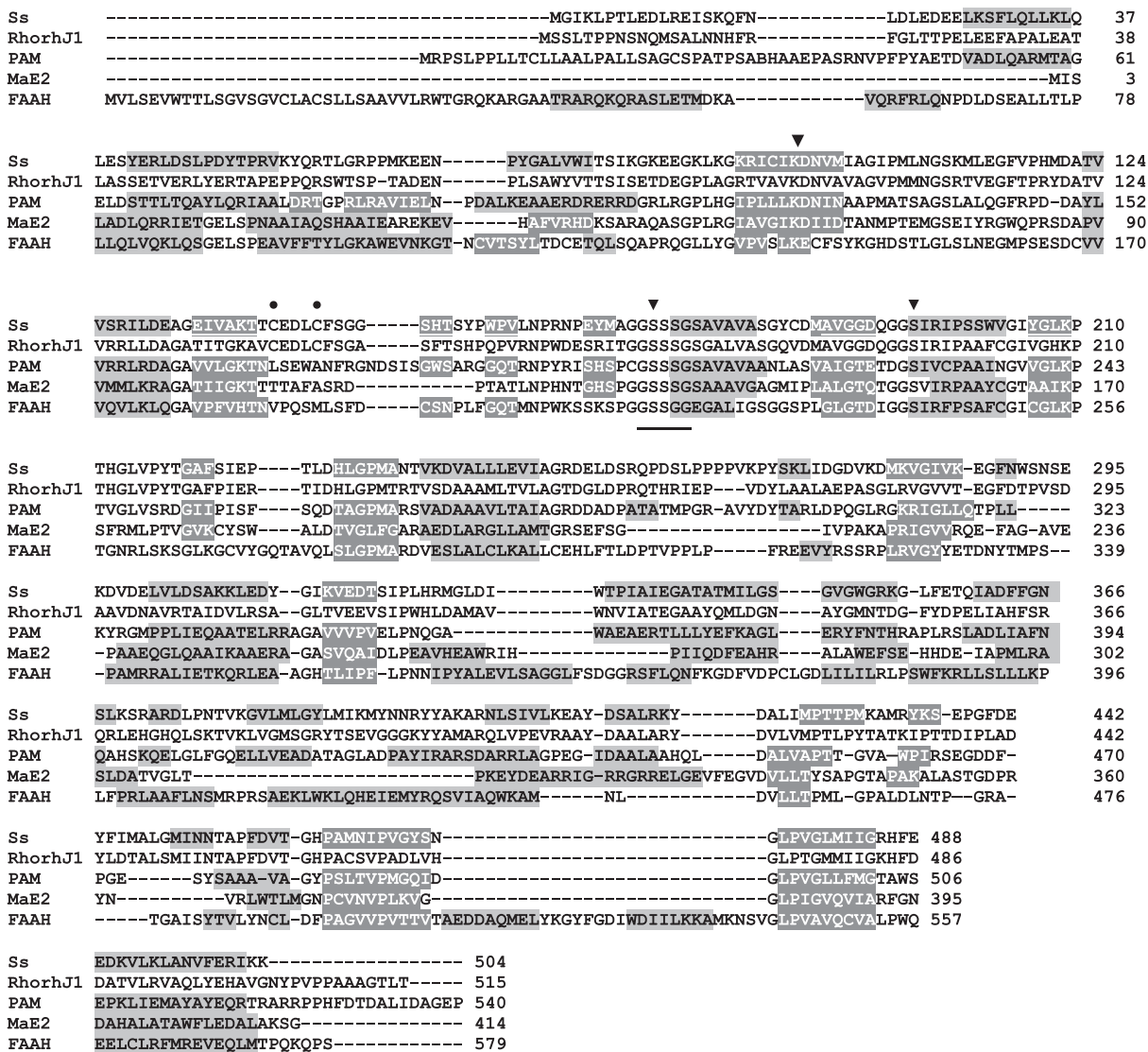


Fig. 1. Multiple sequence alignment of signature AHs. The alignment was manually optimized taking into account the predicted or observed secondary structure also shown. Shaded regions indicate alpha helices (lighter) and beta strands (darker). The conserved GX₃SG motif is underlined; identical residues (black triangles) represent the SsAH putative catalytic triad Ser171–cisSer195–Lys96. Black dots indicate the cysteine residues of the CX₃C motif. RhorhJ1, *Rhodococcus rhodochrous* J1; PAM, peptide amide hydrolase; MaE2, malonamidase; FAAH, fatty acid amide hydrolase.

ber of signature AHs, including RhorhJ1-AH and SsAH, both able to cleave nitriles (Fig. 2).

We built a comparative model of SsAH using the program MODELLER with default parameters. In the model (Fig. 3) the Ser171–cisSer195–Lys96 triad is correctly positioned to perform catalysis with the O_γ atom of Ser171 at about 2.8 Å from the O_γ atom of Ser195 and about 2.7 Å from the amino group of Lys96.

The analysis of the structural model reveals that Cys145, present both in SsAH and in RhorhJ1-AH, is in an ideal position to function as primary nucleophile in a second catalytic triad (Cys145–Ser171–Lys96) that could be responsible for the hydrolysis of nitriles. Indeed, the sulfur atom of Cys145 is at about 3 Å from the O_γ atom of Ser171 and 2.5 Å from the amino group of Lys96 (Fig. 4). This putative alternative triad is located in a different plane from the active site

		141	145		171
P95896	PHMDATVVSRLDEAGEIVAKTTCEDL	CFSGGSHTSY	PWPVLPNPRNPEY	MAGGSSSSGSAV	177
AAO55930	PSEDATVVKRLLAAGATVVGKSVCE	DLCFSGASFTS	SAGAVKNP	WDLARNAGGSSSSGSAV	177
ZP_00124054	PSEDATVVKRLLAAGATVIGKSVCE	DLCFSGASFTS	ATGAVKNP	WDLTRNAGGSSSSGSAV	177
BAC99079	PSRDATVVTLLAAGATVAGKAVCE	DLCFSGSSFT	PASGPVRNP	WDRQREAGGSSSSGSAV	177
CAD36560	PSRDATVVTLLAAGATVAGKAVCE	DLCFSGSSFT	PASGPVRNP	WDRQREAGGSSSSGSAV	177
S38270	PRYDATVVRLLDAGATITGKAVCE	DLCFSGASFTS	HQPVRNP	WDESRTITGGSSSSGSAV	177
P27765	PGFDATVVTLLDAGATILGKATCE	EHYCLSGGSHT	SDPAPVHN	PHRHGYASGGSSSSGSAV	179
YP_046288	PEYDATIVTRMLDAGATILGKATCE	EHFCLSGGSHT	SDPVAVHN	PHYRHGYASGGSSSSGSAV	177
NP_766838	PDFDATIVTRMLDAGAEIKGKVHCE	HFCLSGGSHT	TGSPVHN	PHKMGYSAGGSSSSGSAV	177
ZP_00186529	PEFDATIVTRILDAGGEISGKAVCE	HLCFSGGSHT	SDTGPVLPN	PHDRTRSAGGSSSSGSAV	177
	* **:* * *:* .. : .* ** .*:**.*.* .* ** :****.*..				

Fig. 2. The Cys₃Cys motif is conserved in a restricted group of signature amidases. Partial alignment of amidase sequences containing a second CX₃C motif. From top to bottom (with database accession numbers in parentheses): *Sulfolobus solfataricus* (P95896); *Pseudomonas syringae* pv. tomato str. DC3000 (AAO55930); *Pseudomonas syringae* pv. syringae B728a (ZP_00124054); *Rhodococcus globerulus* (BAC99079); *Rhodococcus erythropolis* (CAD36560); is the *Rhodococcus rhodochrous* J1 (S38270); *Pseudomonas chlororaphis* (P27765); *Acinetobacter* sp. ADP1 (YP_046288); *Bradyrhizobium japonicum* USDA 110 (NP_766838); *Rubrobacter xylanophilus* DSM 9941 (ZP_00186529).

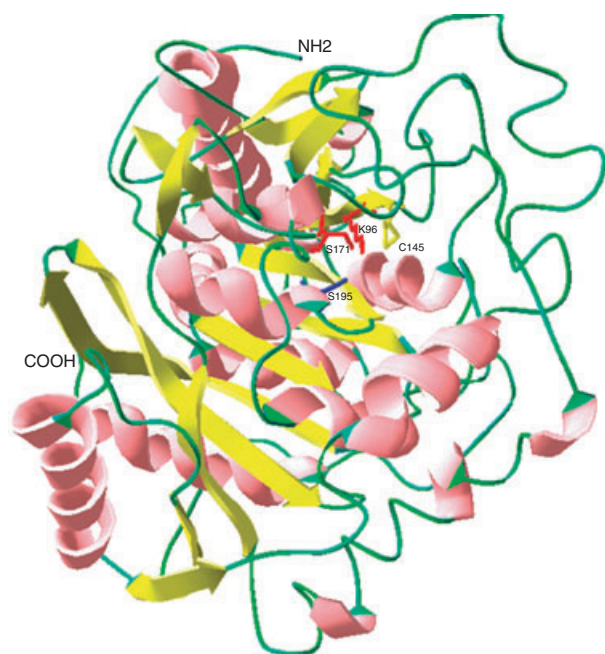


Fig. 3. The homology model of CX₃C signature amidase from *S. solfataricus*. The side chains of the putative catalytic residues are shown. Ser171 and Lys96, shared by the two triads are in red.

catalytic triad and forms an angle of about 107° with its plane (Fig. 5A).

Homology models can be useful to suggest functional hypothesis especially when they are based on a convincing evolutionary relationship, as in this case. Nevertheless their conclusions need to be experimentally verified.

In order to validate our hypothesis, we screened the activity of more than 40 SsAH mutants. The mutants were obtained by random, PCR-mediated mutagenesis and their activity assayed with the colorimetric method of Berthelot, appropriately modified for the assay conditions of the archaeal enzyme. This assay is based on

the measurement of the colour that develops upon ammonia production in the reaction. Ammonia is produced, in stoichiometrical amounts, upon substrate hydrolysis.

Eight of the 40 mutants could hydrolyse most nitriles more efficiently than SsAH-WT. The only amino acid substitution shared by all these mutants was the K96R mutation. To investigate the role of this mutation, we constructed the SsAH-K96R single mutant by site-directed mutagenesis. The 310-nucleotide fragment of the gene encoding SsAH was cut and used as template to introduce, by PCR, the mutation K96R. After amplification the fragment was purified and subcloned into pET3d vector and DNA sequenced for confirmation. The resulting plasmid was used to transform *E. coli* BL21(DE3) cells and the enzyme was expressed by isopropyl thio-β-D-galactoside (IPTG) induction as for the wild-type enzyme. Both SsAH-WT and SsAH-K96R were purified in a similar way and an identical protein concentration was used to compare their nitrilase activity. The SsAH-K96R retains the ability to hydrolyse amides but hydrolyses nitriles more efficiently than the SsAH-WT (Table 1).

The behaviour of this mutant can be rationally explained on the basis of the homology model, as the increased occupancy deriving from the arginine side chain in position 96 might modulate the size of the cleavable substrates (Fig. 4). Furthermore, the amino group of Arg96 could coordinate a water molecule that would be positioned sufficiently close to Cys145 to take part in the catalytic mechanism, thereby increasing the catalytic efficiency of the enzyme for nitrile substrates (Fig. 5B). The model suggests that this putative additional water molecule cannot be accommodated in the structure of SsAH-WT (Fig. 5C). Structural analysis of the model suggests that Arg96 may contribute more effectively than Lys96 to the catalytic mech-

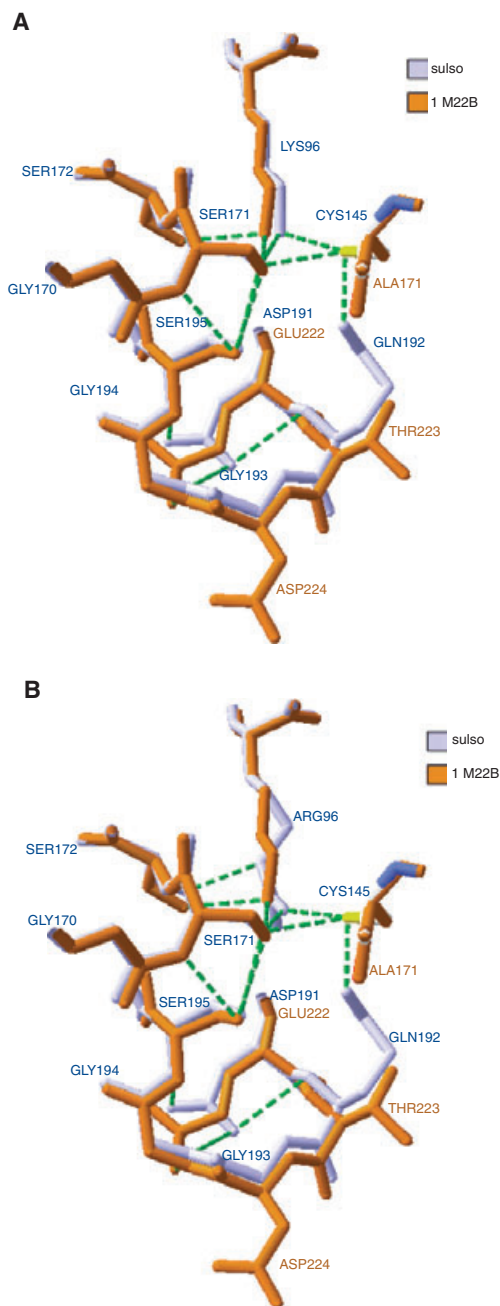


Fig. 4. Comparison between the putative catalytic sites of the SsAH-WT and SsAH-K96R models with those of the peptide amide hydrolase 1M22 template. The figure shows (in blue) the putative catalytic pocket of the SsAH-WT (A) and SsAH-K96R model (B) superimposed to the catalytic pocket of chain B of the template protein (orange). Both models show the Cys145Ala, Asp191Gln and Gln192Thr substitutions observed in the CX₃C subgroup (SsAH numbering).

anism by activating Ser171 (Fig. 5B). One of its amino groups is about 2.6 Å from the O_γ atom of Ser171 and 2.5 Å from the thiol group of Cys145.

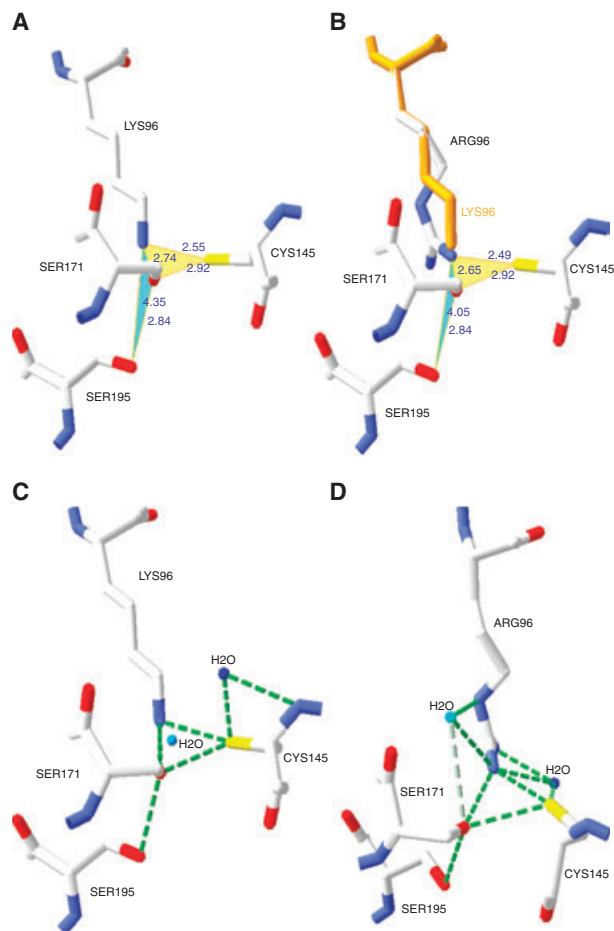


Fig. 5. Closer view of the Ser171–cisSer195–Lys96 (A) and Ser171–Cys145–Lys96 (B) triads. The putatively catalytic triads are located in two different planes forming an angle of about 107°. Putative water molecules and hydrogen bonds in the catalytic site of the SsAH-WT and SsAH-K96R models are shown in (C) and (D), respectively.

Even taking into account all of the limitations of molecular models of proteins with respect to experimental structures, we believe our model to be sufficiently reliable, being based on a respectable sequence similarity, to allow us to formulate the hypothesis that the triad Cys145–Ser171–Lys96 constitutes a second catalytic site. Our experimental analysis of the activity of the mutant SsAH-K96R on aliphatic amides and nitriles strengthens this hypothesis.

Another line of evidence comes from the results of the inhibition studies shown in Fig. 6. Phenylmethanesulfonyl fluoride inhibits amide conversion (more than 94%) and completely suppresses nitrile hydrolysis, supporting the hypothesis that the SsAH nitrilase activity exhibits a typical behaviour of sulphydryl enzymes.

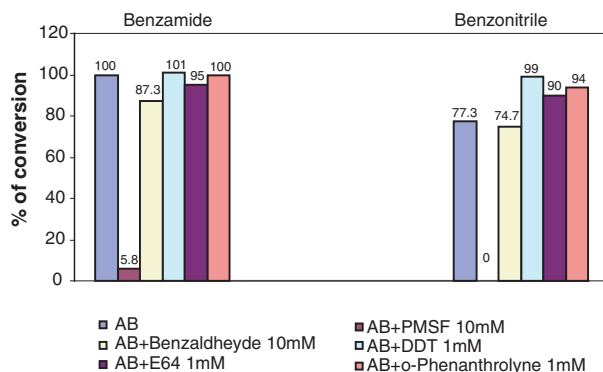


Fig. 6. Inhibition of SsAH by different compounds. AB, assay buffer.

Discussion

The characterization of the SsAH enzyme described here strongly suggests that the Ser171–cisSer195–Lys96 catalytic triad, similarly to other members of this family, forms the active site of this enzyme.

Here we also suggest that a second catalytic triad might exist in this enzyme (and in other members of the family) involving Cys145 as well as Ser171 and Lys96.

Our hypothesis is based on several lines of evidence. A 3D model, built on the basis of a reliable sequence alignment, shows that the members of this second putative triad are in the correct relative orientation. In our model, the O_γ atom of Ser171, the amino group of Lys96 and the thiol group of Cys145 are sufficiently close to each other to form a catalytic site (Fig. 5A).

Second, we isolated eight mutants with a higher catalytic efficiency on nitriles than the wild-type enzyme, and they all share the Lys96Arg mutation. On the basis of our model, this substitution is indeed likely to positively affect the catalytic efficiency. The role of this residue in nitrile catalysis has been confirmed by the construction and characterization of the single Lys96Arg mutant.

Third, inhibition by phenylmethanesulfonyl fluoride suggests that the nitrile hydrolysis activity of the enzyme is likely to be thiol-mediated.

Our proposal of the presence of two different catalytic triads for amide and nitrile substrates is in agreement with the mechanism proposed for nitrilases [13]. These are thiol enzymes that attack the cyano carbon of nitriles (R–C=N) to form a covalent thioimidate complex. Addition of one water molecule is accompanied by release of ammonia and transformation of the planar thioimidate to a planar thiol acyl-enzyme through a tetrahedral intermediate. Addition of a second water molecule allows the acid product to leave and regenerate the enzyme. Pace and Brenner observed that the geometric constraints of this reaction suggest

that nitrilase facilitates interaction with linear ($\approx 180^\circ$) substrate, planar ($\approx 120^\circ$) thioimidate and acyl-enzyme intermediates, and tetrahedral ($\approx 109.5^\circ$) water-bonded intermediate. In contrast, serine and thiol protease and amidase are confined to interacting with planar substrates and tetrahedral intermediates [2].

Our comparative model suggests that the two catalytic triads, with two different nucleophiles, each for a different C–N bond, are positioned in two different planes. When the catalytic base Lys96 is replaced by the chemically similar, but larger, arginine residue, the mutant enzyme hydrolyses only linear substrates, but is able to cleave the triple C–N bond more efficiently than the wild-type enzyme. Our model is able to explain this behaviour, as the arginine can coordinate a second water molecule (Fig. 5D).

Notably, the putative catalytic cysteine is conserved in RhorhJ1-AH, another member of the family known to cleave amide/nitrile substrates. It is likely that other, not yet characterized, members of the family, containing the Cys141X₃Cys145 motif also have a second, partially overlapping catalytic site, and might share the same enzymatic properties.

Experimental procedures

Wild-type SsAH expression and purification

SsAH-WT was expressed in *E. coli* BL21(DE3)STAR, as previously described [9], and purified by diafiltration. The crude extract was loaded on a Vantage 32 column packed with Q-sepharose F.F. (Pharmacia, Fairfield, CT, USA) at 30 mL·min⁻¹ and equilibrated with 20 mM Tris/HCl pH 8.5. First, the column was washed with 5 vols Tris/HCl 20 mM pH 8.5 (buffer A) and subsequently with 2 vols buffer A + 50 mM NaCl. The active fraction was eluted with buffer A + 0.25 M NaCl. The eluted fraction was concentrated in nitrogen to the desired volume with an ultrafiltration cell (Amicon-Millipore mod. 8400; Billerica, MA, USA) equipped with an YM30 membrane. Protein content was determined using the BCA Kit (Pierce, Rockford, IL, USA) or by absorbance at $\lambda = 280$ nm (assuming $E = 0.973$).

Construction and expression of SsAH-K96R mutant

For the random PCR reaction, two oligonucleotide primers were synthesized. Forward and reverse primers correspond to the first 20 nucleotides at the 5'- and 3'- of the gene coding sequence and include the *Nco*I and *Bam*HI sites, at each end, respectively. The 100- μ L PCR reaction contained 1 \times reaction buffer, 1.5 mM MgCl₂, 0.25 mM each dNTP, 0.25 μ M each primer. The amplification was thermocycled

for 30 cycles at 95 °C for 30 s, 50 °C for 30 s, and 72 °C for 90 s with 5 µL of *Taq* polymerase (minicycler MJ research-Genenco MC009904, Bakersfield, CA, USA). After amplification, the DNA fragments were cloned into the pET3d plasmid, purchased from Invitrogen (Carlsbad, CA, USA), and used to transform *E. coli* DH5α grown on Luria–Bertani (LB) containing 100 µg·mL⁻¹ ampicillin. Plasmid DNA was extracted and purified making use of QIAprep (Qiagen, Valencia, CA, USA). The DNA inserts were sequenced by the M-MEDICAL service (<http://www.mmedical.it>).

The *E. coli* BL21(DE3)STAR cells (Stratagene, La Jolla, CA, USA) were transformed with plasmids carrying the mutant genes, in order to screen for nitrile, amide and ester hydrolysis. Each colony was grown in a 50-mL flask containing 20 mL LB medium containing 50 µg·mL⁻¹ ampicillin and 34 µg·mL⁻¹ chloramphenicol. After about 16 h, protein synthesis was induced by adding 0.4 mM IPTG for 2 h. Cells were centrifuged at 5629 *g* for 20 min and cell pellets disrupted (one cycle for 1 min at 40% amplitude) with a cell sonicator (SONICS vibracell™). The recombinant enzyme was purified as described for the wild-type and used at the same protein concentration.

Site-directed mutagenesis

The *SsAH-Lys96Arg* gene was obtained by amplifying a short fragment starting from the initial ATG with the oligonucleotide forward primer: NcoFOR_1, 5'-CTCTCC ATGGGAATTAAGTTACCCACATTGGAGGA-3', carrying the sequence for the *NcoI* restriction site, and a second oligonucleotide reverse primer K96R_rev, 5'-ATATGTAT ACCCGCTATCATCACATTGTCCCTAATGCAAATCC TTTTCC-3', that introduces the A→G substitution in position 287 of the *SsAH* gene. Bstz171. PCR amplification was performed at 95 °C for 30 s, 58 °C for 30 s, and 72 °C for 30 s with 2.5 U of *Taq* polymerase, in 1 × reaction buffer, MgCl₂ 1.5 mM for 24 cycles; dNTP were used each at final concentration of 0.2 mM and oligonucleotides at 0.25 µM, respectively. The amplified DNA fragment was purified from 1.2% agarose gel and, after enzyme digestion, cloned in the pET3d plasmid carrying the *SsAH*-encoding gene previously deleted of the corresponding DNA fragment. After ligation, the plasmid was used to transform in the *E. coli* DH5α cells plated on LB containing ampicillin. The plasmid DNA was extracted and sequenced for confirmation. The plasmid was used to transform *E. coli* BL21(DE3)STAR grown on LB agar containing ampicillin and chloramphenicol. Gene expression was induced by adding 0.4 mM IPTG for 2 h.

All enzymes were from New England Biolabs (Beverly, MA, USA) or Roche (Indianapolis, IN, USA). *Taq* polymerase was from Fermentas (Vilnius, Lithuania) and Euro-Cone (Milan, Italy). Media was LB broth from DIFCO (Franklin Lakes, NJ, USA). Nitriles, amides and corresponding acids were purchased from ACROS (Milan, Italy)

or Sigma Aldrich (St Louis, MO, USA). All other reagents were from Sigma Aldrich, Carlo Erba (Milan, Italy) or Mallinckrodt Baker (Phillipsburg, NJ, USA) and IPTG was from INALCO (Milan, Italy). BCA protein assay KIT and Quany-cleave protease assay kit were from Pierce.

HPLC

Nitriles, amides and acids were analysed by HPLC (Millennium Chromatography Manager equipped with PDA 996, Waters, Milford, MA, USA). An aliquot of 20 µL from the enzyme reaction mix was loaded to the column at a temperature of 40 °C and the molecules eluted with 4.5 mM HClO₄.

Propionamide and its acid were separated with an Rspack KC-811 (MIXED MODE) coupled with Rspack KC-G (Shodex) 8 mm × 300 mm and monitored at 210 nm. Propionic acid was eluted at a flow rate of 1.5 mL·min⁻¹. Benzonitrile, benzamide and benzoic acid were followed by using the Xterra C18 (Waters) column equilibrated with buffer A (20 mM KH₂PO₄ pH 3) and eluted with an isocratic step of 4 min 0% buffer B and 12 min 50% buffer B (methanol). All molecules were monitored at 230 nm or by Refractive Index (1/8 × 10⁻⁵ RIU·T.C. = 0.5).

Enzyme assays

Berthelot assay

Conversion of amides and nitriles was followed by using the Berthelot method [14] optimized for thermophilic enzymes. A 20-mL culture of transformed BL21(DE3) cells were grown overnight and protein synthesis was induced with 0.4 mM IPTG for 2 h. Cells were centrifuged at 6000 r.p.m. for 10 min and resuspended in an appropriate volume of 50 mM Tris/HCl pH 7.2. The suspension was sonicated for 1 min at maximum amplitude and 300 µL of cell crude extract were assayed in standard conditions.

SsAH-WT and SsAH-K96R were used at 60 µg·mL⁻¹ and the acid produced was quantified by the amount of NH₃⁺ produced by reading absorbance of the colour developed at λ = 630 nm.

HPLC assay

Enzyme specific activities were assayed, unless otherwise specified, using 7 µg pure protein incubated for 10 min with 7 mM substrate in assay buffer. One enzyme unit was defined as the amount of enzyme that catalysed the formation of acid (µmol·min⁻¹) at 85 °C. Protein stability at 70 °C was followed for up to 1 week and at 95 °C for 8 h, respectively. Aliquots of the enzyme incubated at fixed temperature, were assayed at different times.

Inhibition of amidase activity

Sixty micrograms of the Ss-AH were incubated at 80 °C in 25 mM phosphate buffer pH 7.4 with 100 µg of benzamide for 30 min and benzonitrile for 16 h. All reactions were carried out in the presence/absence of/ 10 mM phenylmethanesulfonyl fluoride or 10 mM benzaldehyde.

Structural analysis

Primary structure

The primary structure of SsAH was aligned to AHs for which crystallographic or biochemical data were available, using CLUSTALW at the EBI (<http://www.ebi.ac.uk/clustalw/index.html>). Sequences of the rat fatty acid amide hydrolase (1MT5*), peptide amidase (1M22*), malonoamidase E2 (1OCK*), *R. rhodochrous* J1 and *R. erythropolis* N-774 (P22984) and MP50 (Q8KRD8), *Pseudomonas syringae* (v tomato, Q883E3) and *Agrobacterium tumefaciens* (Q9AHE8) were retrieved from the SwissProt Data Base [15].

Secondary structure

Several different methods for the prediction of secondary structures were used (NNPREDICT [16]; PROF [17]; PSPRED [18]). The consensus secondary structure prediction of each protein was used to manually refine the multiple sequence alignment.

3D model

The 3D structure was built using the modelling package MODELLER, using the templates available from the PDB database, and analysed using RASMOL [20], VEGA [21] or SWISSPDBVIEWER [22]. Models were optimized and evaluated using ESPRED3D [23]. Multiple sequence alignments were obtained by combining, weighting and screening the results of several multiple alignment programs.

The 3D model of the SsAH-K96R mutant was obtained from the 3D model of SsAH-WT by replacing the lysine residue with an arginine using SWISSPDBVIEWER 3.7 (SP5). Some torsional space exploration of the side chain was necessary to avoid clashes with the Nδ2 atom of Asn98.

Acknowledgements

This work is part of the 'FANS' project N°2881 funded by the Italian Ministry of University and Research.

References

1 Reilly CO & Turner PD, (2003) The nitrilase family of C-N hydrolyzing enzymes—a comparative study. *J Appl Microbiol* **95**, 1161–1174.

- 2 Pace HC & Brenner C (2001) The nitrilase superfamily: classification, structure and function. *Gen Biol* **2**, 1–9.
- 3 Brenner C (2002) Catalysis in the nitrilase superfamily. *Curr Opin Struct Biol* **12**, 775–782.
- 4 Kobayashi M, Fujiwara Y, Goda M, Komeda H & Shimizu S, (1997) Identification of active sites in amidase: evolutionary relationship between amide bond and peptide bond-cleaving enzymes. *Proc Natl Acad Sci USA* **94**, 11986–11991.
- 5 Chebrou H, Bigey F, Arnaud A & Galzy P, (1996) Study of the amidase signature group. *Bioch Bioph Acta* **1298**, 285–293.
- 6 Shin S, Lee T-H, Ha N-C, Koo HM, Kim S-Y, Lee H-S, Kim YS & Oh B-H (2002) Structure of malanomidase E2 reveals a novel Ser-cisSer-Lys catalytic triad in a new serine hydrolase fold that is prevalent in nature. *EMBO J* **21**, 2509–2516.
- 7 Neumann S, Granzin J, Kula M-R & Labahn J, (2002) Crystallization and preliminary X-ray data of the recombinant peptide amidase from *Stenotrophomonas maltophilia*. *Acta Crystallogr Sect D* **58**, 333–335.
- 8 Bracey MH, Hanson MA, Masuda KR, Stevens RC & Cravatt BF, (2002) Structural adaptations in a membrane enzyme that terminates endocannabinoid signaling. *Science* **298**, 1793–1796.
- 9 Scotto d'Abusco A, Ammendola S, Scandurra R & Politi L (2001) Molecular and biochemical characterization of the recombinant amidase from hyperthermophilic archaeon *Sulfolobus solfataricus*. *Extremophiles* **5**, 183–192.
- 10 Kobayashi M, Komeda H, Nagasawa T, Nishiyama M, Horinouchi S, Beppu T, Yamada H & Shimizu S (1993) Amidase coupled with low-molecular-mass nitrile hydratase from *Rhodococcus rhodochrous* J1. *Eur J Biochem* **217**, 327–336.
- 11 Kobayashi M, Goda M & Shimizu S (1998) The catalytic mechanism of amidase also involves nitrile hydrolysis. *FEBS Lett* **439**, 325–328.
- 12 McKinney MK & Cravatt BF (2003) Evidence for distinct roles in catalysis for residues of the serine-serine-lysine catalytic triad of fatty acid amide hydrolase. *Biochemistry* **278**, 37393–37399.
- 13 Stevenson DE, Feng R, Dumas F, Groleau D, Mihoc A & Storer AC (1992) Mechanistic and structural studies on *Rhodococcus* ATCC39484 nitrilase. *Biotechnol Appl Biochem* **15**, 283–302.
- 14 Banerjee A, Sharma R & Banerjee UC (2003) A rapid and sensitive fluorometric assay method for the determination of nitrilase activity. *Biotechnol Appl Biochem* **37**, 289–293.
- 15 Altschul SF, Madden TL, Schaffer AA, Zhang J, Zhang Z, Miller W & Lipman DJ (1997) Gapped BLAST and PSI-BLAST: a new generation of protein database search programs. *Nucleic Acids Res* **25**, 3389–3402.

- 16 Kneller DG, Cohen FE & Langridge R (1990) Improvements in protein secondary structure prediction by an enhanced neural network. *J Mol Biol* **214**, 171–182.
- 17 Ouali M & King RD (2000) Cascaded multiple classifiers for secondary structure prediction. *Prot Sci* **9**, 1162–1176.
- 18 McGuffin LJ, Bryson K & Jones DT (2000) The PSIPRED protein structure prediction server. *Bioinformatics* **16**, 404–405.
- 19 Sayle RA & Milner-White EJ (1995) RasMol: Biomolecular graphics for all. *Trends Biochem Sci* **20**, 374–376.
- 20 Pedretti A, Villa L & Vistoli G (2003) VEGA: a versatile program to convert, handle and visualize molecular structure on Windows-based PC. *J Mol Graph* **21**, 47–49.
- 21 Peitsch MC (1996) ProMod and Swiss-Model: Internet-based tools for automated comparative protein modeling. *Biochem Soc Trans* **24**, 274–279.
- 22 Jones DT (1999) Protein secondary structure prediction based on position-specific scoring matrices. *J Mol Biol* **292**, 195–202.
- 23 Lambert C, Leonard N, De Bolle X & Depiereux E (2002) ESyPred3D: prediction of proteins' 3D structures. *Bioinformatics* **18**, 1250–1256.